J. Appl. Comput. Mech., 7(2) (2021) 505-519
DOI: 10.22055/JACM.2020.35328.2628

ISSN: 2383-4536
jacm.scu.ac.ir

Shahid Chamran University of Ahvaz

Journal of Applied and Computational Mechanics

Research Paper

Free Vibration Analysis of FG Porous Sandwich Plates under Various Boundary Conditions

Lazreg Hadji[1,2], Mehmet Avcar[3]

[1] University of Tiaret, Department of Mechanical Engineering, BP 78 Zaaroura, Tiaret,14000, Algeria, Email: had_laz@yahoo.fr

[2] University of Tiaret, Laboratory of Geomatics and Sustainable Development, Tiaret, 14000, Algeria

[3] Suleyman Demirel University, Department of Civil Engineering, Isparta, 32260, Turkey, Email: mehmetavcar@sdu.edu.tr

Received October 07 2020; Revised November 12 2020; Accepted for publication November 15 2020.
Corresponding author: Mehmet Avcar (mehmetavcar@yahoo.com)

Abstract. In the present work, free vibration analysis of the square sandwich plate with functionally graded (FG) porous face sheets and isotropic homogenous core is performed under various boundary conditions. For this purpose, the material properties of the sandwich plate are supposed to vary continuously through the thickness direction according to the volume fraction of constituents defined with the modified rule of the mixture including porosity volume fraction with three different types of porosity distribution over the cross-section. Furthermore, a hyperbolic shear displacement theory is used in the kinematic relation of the FG porous sandwich plate, and the equations of motion are derived utilizing Hamilton's principle. Analytical solutions are achieved for free vibration analysis of square sandwich plates with FG porous face sheets under various boundary conditions, i.e. combinations of clamped (C), simply supported (SS), and free (F) edges are presented. Several parametrical studies are conducted to examine the effects of porosity volume fraction, type of porosity distribution model, lay-up scheme, side to thickness ratio, and boundary conditions on the free vibration of the FG sandwich plates. Finally, it is concluded that the investigated parameters have significant effects on the free vibration of the FG sandwich plates and the negative effects of porosity may be reduced by adopting suitable values for said parameters, considerably.

Keywords: Functionally graded materials, Sandwich plates, Porosity, Free vibration, Boundary conditions.

1. Introduction

Functionally graded materials (FGMs) are advanced nonhomogeneous composites composed of different phases of constituents (generally ceramic and metal), namely the material properties of FGMs vary unidirectional (through-thickness or length) or bi-directional (both through-thickness and length) gradually and continuously depending on a function with the purpose of the desired tasks. FGMs have comprehensive applications in the fields of aerospace, medicine, defense, energy, optoelectronics, automotive, biotechnology, aviation, civil, and mechanical engineering structures [1-10].

Sandwich structures are a special type of composite materials which are composed of one core to bonded two layers, and they have been used in many engineering fields such as spacecraft, aircraft, railway, and car structures, wind turbine blades, boat or ship superstructures, thanks to their impressive properties i.e. high stiffness to weight ratio [11]. Sandwich structures could be designed in various ways, in which the use of FGMs increasing day by day due to FGMs offers smooth, gradually, and continuous variation of material properties from one surface to another and by this way increasing stress levels, matrix cracks, and delamination failure can be eliminated in sandwich structures. Therefore, the examination of the mechanical behaviors of FG sandwich structures has been an interesting issue for scientists. Zenkour [12, 13] presented the bending, buckling, and vibration analyses of simply supported FG sandwich plates. Zenkour and Sobhy [14] studied the sinusoidal shear deformation plate theory to study the thermal buckling of FG sandwich plates. El Meiche et al. [15] proposed a hyperbolic shear deformation theory taking into account transverse shear deformation effects for the buckling and free vibration analysis of thick FG sandwich plates. Mohammadi and Khalili [16] analyzed the free vibration of sandwich plates with power-law FG face sheets in different thermal environments. Bessaim et al. [17] developed a higher-order shear and normal deformation theory for the bending and free vibration analysis of sandwich plates with FG isotropic face sheets. Thai et al. [18] suggested a first-order shear deformation theory for FG sandwich plates composed of FG face sheets and an isotropic homogeneous core. Tlidji et al. [19] examined the thermomechanical bending response of functionally graded sandwich plates using a four-variable refined plate theory. Yang et al. [20] studied the free vibration of the FG sandwich beams by a meshfree boundary-domain integral equation method. Mantari and Granados [21] developed a first shear deformation theory for the static analysis of the FG sandwich plate. Tounsi et al. [22] studied the buckling and vibration analyses of FG sandwich plates using three-unknown non-polynomial shear deformation theory. Ahmadi [23] presented a layerwise formulation based on the Galerkin method to investigate the three-dimensional stress state in

Published online: November 20 2020

a long sandwich plate which is subjected to tension force and pure bending moment. Menasria et al. [24] proposed a new displacement field that includes undetermined integral terms for analyzing the thermal buckling response of FG sandwich plates. Şimşek and Al-Shujairi [25] examined the static, free, and forced vibration of FG sandwich beams under the action of double moving harmonic loads traveling with constant velocities using Timoshenko beam theory. Wang et al. [26] investigated the free vibration of the FG sandwich doubly-curved panels and shells of revolution with arbitrary boundary conditions. Dash et al. [27] studied the modal frequency responses of FG sandwich doubly curved shell panels using a higher-order finite element formulation. Raissi et al. [28] examined the effects of functional properties of the face sheets as well as the mechanical properties of the core and other constituents, on stress distribution in a simply supported five-layer sandwich plate. Rezaiee-Pajand et al. [29] developed a mixed interpolated formulation for nonlinear analysis of FG sandwich plates and shells. Meksi et al. [30] introduced a shear deformation plate theory to examine the bending, buckling, and free vibration responses of FG sandwich plates. Nam and Kien [31] investigated the free vibration of FG sandwich plates partially supported by a Pasternak elastic foundation.

Throughout the production of FGMs some technical problems such as the major difference in solidification temperatures between material constituents during sintering, and production of samples of FGMs using a multi-step sequential infiltration technique could cause porosities in FGMs and so the mechanical properties of FGMs may change noticeably [32]. Thus, the effect of the porosity on the FGMs is an important problem and must be investigated for the safe design of FG structures. Therefore, the investigation of the mechanical behaviors of porous FG structures became a hot topic for scientists in recent years. Wattanasakulpong and Ungbhakorn [33] studied linear and nonlinear vibration problems of FG porous beams by using a differential transformation method with different kinds of elastically end restrained. Ait Atmane et al. [34] examined the effects of thickness stretching and porosity on the bending, free vibration, and buckling of FG beams resting on elastic foundations. Ebrahimi and Jafari [35] investigated thermomechanical vibration characteristics of FG Reddy beams made of porous material subjected to various thermal loadings investigated utilizing a Navier solution method. Akbaş [36-40] examined different mechanical behaviors of FG porous plates, beams, and nanorods in detail. Zouatnia et al. [41] developed an analytical solution for bending and vibration responses of FG beams with porosities. Arshid and Khorshidvand [42] studied the free vibration analysis of a circular plate made up of a porous material integrated by piezoelectric actuator patches. Wu et al. [43] introduced a finite element method framework to study the free and forced vibrations of FG porous beam-type structures. Avcar [44] investigated the free vibration of imperfect sigmoid and power-law FG beams using classical and first order shear deformation beam theories. Chen et al. [45] dealt with the buckling and bending of analyses of the FG porous plate using the Chebyshev-Ritz method. Jalaei and Civalek [46] examined the dynamic instability of viscoelastic porous FG nanobeam embedded on visco-Pasternak medium subjected to an axially oscillating loading as well as magnetic field. Nguyen et al. [47] presented an isogeometric Bézier finite element formulation for bending and transient analysis of FG porous plates reinforced by graphene platelets embedded in piezoelectric layers. Arefi et al. [48] investigated the size-dependent deflection analysis of FG graphene nanoplatelets reinforced composite micro-plates with porosity subjected to transverse load. Mashat et al. [49] dealt with the impacts of temperature and moisture on the bending behavior of FG porous plates resting on elastic foundations. Zine et al. [50] examined the bending response of FG porous plates using a cubic shear deformation theory.

In recent years, scientists have also handled the examination of the mechanical behaviors of FG porous sandwich structures, however, the number of studies on this topic is still limited. Chen et al. [51] examined the nonlinear free vibration behavior of shear deformable FG porous sandwich beam. Rezaei and Saidi [52] studied free vibration analysis of Levy-type thick rectangular porous–cellular plates using Carrera unified formulation. Fazzolari [53] investigated the free vibration and elastic stability behavior of three dimensional FG sandwich beams featured by two different types of porosity, with arbitrary boundary conditions and resting on Winkler-Pasternak elastic foundations. Fu et al. [54] focused on sound transmission loss analysis of corrugated core FG sandwich plates filled with a porous material, wherein two types of FGM sandwich structures are considered, which include one with FGM face sheets and homogeneous ceramic or metal core, and the other with FGM core and homogeneous face sheets. Zenkour [55] studied the bending responses of FG porous single-layered and sandwich thick rectangular plates according to a quasi-3D shear deformation theory. Daikh and Zenkour [56] proposed a porosity distribution for bending analysis of the model of FGM sandwich plates. Heshmati and Jalali [57] investigated the free vibration of sandwich circular and annular plates with a core made of materials with functionally graded porosity. Keddouri et al. [58] introduced a new displacement-based high-order shear deformation theory for the static response of the FG porous sandwich plate. Rahmani et al. [59] investigated the vibration behavior of two types of porous FG circular sandwich plates applying a modified high order sandwich plate theory. Trinh et al. [60] presented the fundamental frequencies and nonlinear dynamic responses of FG sandwich shells with double curvature under the influence of thermomechanical loadings and porosities. Adhikari et al. [61] intended to model the effect of porosity type defect and analyzed the consequences of porosity on the buckling characteristic of various types of FG sandwich combinations. Hadji [62] proposed a higher order shear deformation model for static analysis of functionally graded beams with considering porosities. Wang et al. [63] developed a high-order shear deformable beam model for examining the transient response of a sandwich porous beam when acted upon by a non-uniformly distributed moving mass. Zhang et al. [64] presented the free vibration and damping analysis of porous FG sandwich plates based on a modified Fourier-Ritz method.

This study presents the free vibration analysis of the square sandwich plate with FG porous faces and homogenous ceramic core considering various boundary conditions. For this aim, the material properties of the sandwich plate are supposed to vary continuously through the thickness direction according to the volume fraction of constituents defined with the modified rule of the mixture including porosity volume fraction with three different types of porosity distribution over the cross-section. Furthermore, a hyperbolic shear displacement theory is used in the kinematic relation of the FG porous sandwich plate, and the equations of motion are derived utilizing Hamilton's principle. Analytical solutions are gotten for the free vibration analysis of square sandwich plates with FG porous layers under various boundary conditions, i.e. combinations of clamped (C), simply supported(S), and free (F) edges are presented. Several parametrical studies are performed for examining the effects of the porosity volume fraction, type of porosity distribution model, lay-up scheme, side to thickness ratio, and boundary conditions on the free vibration of the FG sandwich plates.

2. The Formulation of the Problem

Consider a square sandwich FG plate with FG porous faces and homogenous ceramic core as shown in Fig. 1, where a, $b=a$ and h shows the dimensions of the sandwich plate in the X, Y, and Z directions, respectively. The Cartesian coordinate system O(X,Y,Z) is placed on the left edge of the central axis of the sandwich plate, the edges are parallel to the x and y axes and the top and bottom faces are located at $z = \pm h/2$.

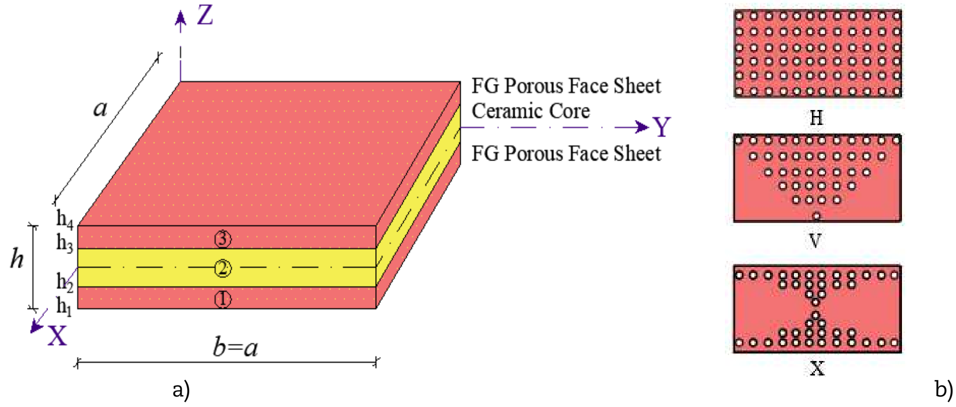

Fig. 1. a) The geometry of the sandwich plate with FG porous faces and ceramic core b) The porosity models

The sandwich plate is composed of three layers, a homogenous ceramic core, and two FG porous face sheets. The material properties of the face sheets vary from metal to ceramic and the core is made of ceramic. The volume fraction of the faces and core varies according to the following power-law function through the thickness of the sandwich plate

$$\begin{aligned} &V^{(1)}(Z)=\left(\frac{Z-h_1}{h_2-h_1}\right)^k \quad h_1\le Z\le h_2\\ &V^{(2)}(Z)=1 \qquad\qquad h_2\le Z\le h_3\\ &V^{(3)}(Z)=\left(\frac{Z-h_4}{h_3-h_4}\right)^k \quad h_3\le Z\le h_4\end{aligned} \tag{1}$$

where h_1, h_2, and h_3 and h_4 are the values of thickness and shown on Fig 1. Coordinates of bottom face and k indicates the power-law coefficient (volume fraction index). Note that, as k=0, the material properties of the sandwich plate transform into homogenous ceramic. Fig. 1b shows three different distribution models for the porosity in FG layers i.e. homogenous (H), V and X porosity distributions. According to these models, the effective material properties (P) for each layer are given as follows

For homogeneous porosity distribution:

$$\begin{aligned} &P^{(1)}(Z)=P_m+(P_c-P_m)V^{(1)}(Z)-\frac{\xi}{2}(P_c+P_m)\\ &P^{(2)}(Z)=P_m+(P_c-P_m)V^{(2)}(Z)\\ &P^{(3)}(Z)=P_m+(P_c-P_m)V^{(3)}(Z)-\frac{\xi}{2}(P_c+P_m)\end{aligned} \tag{2}$$

For X porosity distribution:

$$\begin{aligned} &P^{(1)}(Z)=P_m+(P_c-P_m)V^{(1)}(Z)-\frac{\xi}{2}(P_c+P_m)\left|\frac{2Z-(h_1+h_2)}{h_1-h_2}\right|\\ &P^{(2)}(Z)=P_m+(P_c-P_m)V^{(2)}(Z)\\ &P^{(3)}(Z)=P_m+(P_c-P_m)V^{(3)}(Z)-\frac{\xi}{2}(P_c+P_m)\left|\frac{2Z-(h_3+h_4)}{h_3-h_4}\right|\end{aligned} \tag{3}$$

For V porosity distribution:

$$\begin{aligned} &P^{(1)}(Z)=P_m+(P_c-P_m)V^{(1)}(Z)-\frac{\xi}{2}(P_c+P_m)\left(\frac{Z-h_2}{h_1-h_2}\right)\\ &P^{(2)}(Z)=P_m+(P_c-P_m)V^{(2)}(Z)\\ &P^{(3)}(Z)=P_m+(P_c-P_m)V^{(3)}(Z)-\frac{\xi}{2}(P_c+P_m)\left(\frac{Z-h_4}{h_3-h_4}\right)\end{aligned} \tag{4}$$

where ξ denotes the volume fraction of porosity. Based on the higher-order shear deformation plate theory, the displacement fields of the plate are presented as follows (Chikr et al. 2020)

$$\begin{aligned} &u(x,y,z,t)=u_0(x,y,t)-z\frac{\partial w_b}{\partial x}-f(z)\frac{\partial w_s}{\partial x}\\ &v(x,y,z,t)=v_0(x,y,t)-z\frac{\partial w_b}{\partial y}-f(z)\frac{\partial w_s}{\partial y}\\ &w(x,y,z,t)=w_b(x,y,t)+w_s(x,y,t)\end{aligned} \tag{5}$$

where, u, v, and w are the displacements in X, Y, and Z directions, respectively. Note that, Eq. (5) introduces only four unknowns (u_0, v_0, w_b, and w_s). In Eq. (5), $f(z)$ can be defined using the higher-order shear deformation plate as follows

$$f(z) = \frac{3}{2}\pi h \tanh\left(\frac{z}{h}\right) - \frac{3}{2}\pi z \operatorname{sech}\left(\frac{1}{2}\right)^2 \tag{6}$$

The nonzero strains associated with the displacement field in Eq. (5) are:

$$\begin{Bmatrix} \varepsilon_x \\ \varepsilon_y \\ \gamma_{xy} \end{Bmatrix} = \begin{Bmatrix} \varepsilon_x^0 \\ \varepsilon_y^0 \\ \gamma_{xy}^0 \end{Bmatrix} + z \begin{Bmatrix} k_x^b \\ k_y^b \\ k_{xy}^b \end{Bmatrix} + f(z) \begin{Bmatrix} k_x^s \\ k_y^s \\ k_{xy}^s \end{Bmatrix} \tag{7}$$

$$\begin{Bmatrix} \gamma_{yz} \\ \gamma_{xz} \end{Bmatrix} = g(z) \begin{Bmatrix} \gamma_{yz}^s \\ \gamma_{xz}^s \end{Bmatrix} \tag{8}$$

where

$$\begin{Bmatrix} \varepsilon_x^0 \\ \varepsilon_y^0 \\ \gamma_{xy}^0 \end{Bmatrix} = \begin{Bmatrix} \dfrac{\partial u_0}{\partial x} \\ \dfrac{\partial v_0}{\partial x} \\ \dfrac{\partial u_0}{\partial y} + \dfrac{\partial v_0}{\partial x} \end{Bmatrix}, \begin{Bmatrix} k_x^b \\ k_y^b \\ k_{xy}^b \end{Bmatrix} = \begin{Bmatrix} -\dfrac{\partial^2 w_b}{\partial x^2} \\ -\dfrac{\partial^2 w_b}{\partial y^2} \\ -2\dfrac{\partial^2 w_b}{\partial x \partial y} \end{Bmatrix}$$

$$\begin{Bmatrix} k_x^s \\ k_y^s \\ k_{xy}^s \end{Bmatrix} = \begin{Bmatrix} -\dfrac{\partial^2 w_s}{\partial x^2} \\ -\dfrac{\partial^2 w_s}{\partial y^2} \\ -2\dfrac{\partial^2 w_s}{\partial x \partial y} \end{Bmatrix}, \begin{Bmatrix} \gamma_{yz}^s \\ \gamma_{xz}^s \end{Bmatrix} = \begin{Bmatrix} \dfrac{\partial w_s}{\partial y} \\ \dfrac{\partial w_s}{\partial x} \end{Bmatrix} \tag{9}$$

and

$$g(z) = 1 - \frac{df(z)}{dz} \tag{10}$$

The constitutive relations can be expressed for elastic and isotropic FGMs as

$$\begin{Bmatrix} \sigma_x \\ \sigma_y \\ \tau_{xy} \\ \tau_{yz} \\ \tau_{xz} \end{Bmatrix} = \begin{bmatrix} C_{11} & C_{12} & 0 & 0 & 0 \\ C_{12} & C_{22} & 0 & 0 & 0 \\ 0 & 0 & C_{66} & 0 & 0 \\ 0 & 0 & 0 & C_{44} & 0 \\ 0 & 0 & 0 & 0 & C_{55} \end{bmatrix} \begin{Bmatrix} \varepsilon_x \\ \varepsilon_y \\ \gamma_{xy} \\ \gamma_{yz} \\ \gamma_{xz} \end{Bmatrix} \tag{11}$$

where $\sigma_x, \sigma_y, \tau_{xy}, \tau_{yz}, \tau_{xz}$ and $\varepsilon_x, \varepsilon_y, \gamma_{xy}, \gamma_{yz}, \gamma_{xz}$ are the components of stress and strain respectively. C_{ij} are the coefficients of stiffness and are defined as

$$C_{11} = C_{22} = \frac{E(z)}{1-\nu^2}, C_{12} = \frac{\nu\, E(z)}{1-\nu^2}, C_{44} = C_{55} = C_{66} = \frac{E(z)}{2(1+\nu)} \tag{12}$$

Hamilton's principle is herein utilized to determine the equations of motion

$$\int_0^t (\delta\, U - \delta\, T)\, dt = 0 \tag{13}$$

where δU and δT are the variations of strain and kinetic energies, respectively. The variation of strain energy of the sandwich plate is given by

$$\begin{aligned} \delta\, U &= \int_V \left[\sigma_x \delta\, \varepsilon_x + \sigma_y \delta\, \varepsilon_y + \tau_{xy} \delta\, \gamma_{xy} + \tau_{yz} \delta\, \gamma_{yz} + \tau_{xz} \delta\, \gamma_{xz} \right] dV \\ &= \int_A \left[N_x \delta\, \varepsilon_x^0 + N_y \delta\, \varepsilon_y^0 + N_{xy} \delta\, \gamma_{xy}^0 + M_x^b \delta\, k_x^b + M_y^b \delta\, k_y^b + M_{xy}^b \delta\, k_{xy}^b + M_x^s \delta\, k_x^s + M_y^s \delta\, k_y^s + M_{xy}^s \delta\, k_{xy}^s + S_{yz}^s \delta\, \gamma_{yz}^s + S_{xz}^s \delta\, \gamma_{xz}^s \right] dA = 0 \end{aligned} \tag{14}$$

The stress resultants N, M and S can be defined as

$$
\begin{aligned}
&\left(N_i, M_i^b, M_i^s\right) = \int_{-h/2}^{h/2} (1, z, f)\sigma_i dz, (i = x, y, xy) \\
&\left(S_{xz}^s, S_{yz}^s\right) = \int_{-h/2}^{h/2} g\left(\tau_{xz}, \tau_{yz}\right) dz
\end{aligned}
\tag{15}
$$

The variation of the kinetic energy of the sandwich plate can be expressed as

$$
\begin{aligned}
\delta T &= \int_{-\frac{h}{2}}^{\frac{h}{2}} \int_{\Omega} [\dot{u}\delta\,\dot{u} + \dot{v}\delta\,\dot{v} + \dot{w}\delta\,\dot{w}]\ \rho(z)\, d\Omega\, dz \\
&= \int_A \Big\{ I_0 \left[\dot{u}_0 \delta\dot{u}_0 + \dot{v}_0\delta\dot{v}_0 + (\dot{w}_b + \dot{w}_s)(\delta\dot{w}_b + \delta\dot{w}_s)\right] \\
&- I_1 \left(\dot{u}_0 \frac{\partial\delta\dot{w}_b}{\partial x} + \frac{\partial\dot{w}_b}{\partial x}\delta\,\dot{u}_0 + \dot{v}_0 \frac{\partial\delta\dot{w}_b}{\partial y} + \frac{\partial\dot{w}_b}{\partial y}\delta\,\dot{v}_0 \right) \\
&- I_2 \left(\dot{u}_0 \frac{\partial\delta\dot{w}_s}{\partial x} + \frac{\partial\dot{w}_s}{\partial x}\delta\,\dot{u}_0 + \dot{v}_0 \frac{\partial\delta\dot{w}_s}{\partial y} + \frac{\partial\dot{w}_s}{\partial y}\delta\,\dot{v}_0 \right) \\
&+ J_1 \left(\frac{\partial\dot{w}_b}{\partial x}\frac{\partial\delta\,\dot{w}_b}{\partial x} + \frac{\partial\dot{w}_b}{\partial y}\frac{\partial\delta\,\dot{w}_b}{\partial y} \right) + K_2 \left(\frac{\partial\dot{w}_s}{\partial x}\frac{\partial\delta\,\dot{w}_s}{\partial x} + \frac{\partial\dot{w}_s}{\partial y}\frac{\partial\delta\,\dot{w}_s}{\partial y} \right) \\
&+ J_2 \left(\frac{\partial\dot{w}_b}{\partial x}\frac{\partial\delta\,\dot{w}_s}{\partial x} + \frac{\partial\dot{w}_s}{\partial x}\frac{\partial\delta\,\dot{w}_b}{\partial x} + \frac{\partial\dot{w}_b}{\partial y}\frac{\partial\delta\,\dot{w}_s}{\partial y} + \frac{\partial\dot{w}_s}{\partial y}\frac{\partial\delta\,\dot{w}_b}{\partial y} \right) \Big\} dA
\end{aligned}
\tag{16}
$$

where dot-superscript convention indicates the differentiation concerning the time variable t, $\rho(z)$ is the mass density, and I_i, J_i and K_i are the mass inertias expressed by

$$
\begin{aligned}
&\left(I_0, I_1, I_2\right) = \int_{-h/2}^{h/2} \left(1, z, z^2\right)\rho(z) dz \\
&\left(J_1, J_2, K_2\right) = \int_{-h/2}^{h/2} \left(f, z\,f, f^2\right)\rho(z) dz
\end{aligned}
\tag{17}
$$

The following expressions are obtained after substituting Eqs. (14) and (16) into Eq. (13)

$$
\begin{aligned}
&\delta\,u_0: \quad \frac{\partial N_x}{\partial x} + \frac{\partial N_{xy}}{\partial y} = I_0\ddot{u}_0 - I_1\frac{\partial\ddot{w}_b}{\partial x} - J_1\frac{\partial\ddot{w}_s}{\partial x} \\
&\delta\,v_0: \quad \frac{\partial N_{xy}}{\partial x} + \frac{\partial N_y}{\partial y} = I_{01}\ddot{v}_0 - I_1\frac{\partial\ddot{w}_b}{\partial y} - J_1\frac{\partial\ddot{w}_s}{\partial y} \\
&\delta\,w_b: \quad \frac{\partial^2 M_x^b}{\partial x^2} + 2\frac{\partial^2 M_{xy}^b}{\partial x\partial y} + \frac{\partial^2 M_y^b}{\partial y^2} = I_0\left(\ddot{w}_b + \ddot{w}_s\right) + I_1\left(\frac{\partial\ddot{u}_0}{\partial x} + \frac{\partial\ddot{v}_0}{\partial y}\right) - I_2\nabla^2\ddot{w}_b - J_2\nabla^2\ddot{w}_s \\
&\delta\,w_s: \quad \frac{\partial^2 M_x^s}{\partial x^2} + 2\frac{\partial^2 M_{xy}^s}{\partial x\partial y} + \frac{\partial^2 M_y^s}{\partial y^2} + \frac{\partial S_{xz}^s}{\partial x} + \frac{\partial S_{yz}^s}{\partial y} = I_0\left(\ddot{w}_b + \ddot{w}_s\right) + J_1\left(\frac{\partial\ddot{u}_0}{\partial x} + \frac{\partial\ddot{v}_0}{\partial y}\right) - J_2\nabla^2\ddot{w}_b - K_2\nabla^2\ddot{w}_s
\end{aligned}
\tag{18}
$$

Substituting Eqs. (8) into Eq. (11) and the subsequent results into Eqs. (15), the stress resultants are obtained in terms of strains as following compact form:

$$
\begin{Bmatrix} N \\ M^b \\ M^s \end{Bmatrix} = \begin{bmatrix} A & B & B^s \\ B & D & D^s \\ B^s & D^s & H^s \end{bmatrix} \begin{Bmatrix} \varepsilon \\ k^b \\ k^s \end{Bmatrix}, S = A^s\gamma
\tag{19}
$$

in which

$$
N = \left\{N_x, N_y, N_{xy}\right\}^t,\ M^b = \left\{M_x^b, M_y^b, M_{xy}^b\right\}^t, M^s = \left\{M_x^s, M_y^s, M_{xy}^s\right\}^t
\tag{20}
$$

$$
\varepsilon = \left\{\varepsilon_x^0, \varepsilon_y^0, \gamma_{xy}^0\right\}^t, k^b = \left\{k_x^b, k_y^b, k_{xy}^b\right\}^t, k^s = \left\{k_x^s, k_y^s, k_{xy}^s\right\}^t
\tag{21}
$$

$$
A = \begin{bmatrix} A_{11} & A_{12} & 0 \\ A_{12} & A_{22} & 0 \\ 0 & 0 & A_{66} \end{bmatrix}, B = \begin{bmatrix} B_{11} & B_{12} & 0 \\ B_{12} & B_{22} & 0 \\ 0 & 0 & B_{66} \end{bmatrix}, D = \begin{bmatrix} D_{11} & D_{12} & 0 \\ D_{12} & D_{22} & 0 \\ 0 & 0 & D_{66} \end{bmatrix}
\tag{22}
$$

$$B^s=\begin{bmatrix} B^s_{11} & B^s_{12} & 0 \\ B^s_{12} & B^s_{22} & 0 \\ 0 & 0 & B^s_{66}\end{bmatrix}, D^s=\begin{bmatrix} D^s_{11} & D^s_{12} & 0 \\ D^s_{12} & D^s_{22} & 0 \\ 0 & 0 & D^s_{66}\end{bmatrix}, H^s=\begin{bmatrix} H^s_{11} & H^s_{12} & 0 \\ H^s_{12} & H^s_{22} & 0 \\ 0 & 0 & H^s_{66}\end{bmatrix} \tag{23}$$

$$S=\left\{S^s_{xz}, S^s_{yz}\right\}^t, \gamma=\left\{\gamma^0_{xz}, \gamma^0_{yz}\right\}^t, A^s=\begin{bmatrix} A^s_{44} & 0 \\ 0 & A^s_{55}\end{bmatrix} \tag{24}$$

and the stiffness components are

$$\begin{aligned}
&\begin{Bmatrix} A_{11} & B_{11} & D_{11} & B^s_{11} & D^s_{11} & H^s_{11} \\ A_{12} & B_{12} & D_{12} & B^s_{12} & D^s_{12} & H^s_{12} \\ A_{66} & B_{66} & D_{66} & B^s_{66} & D^s_{66} & H^s_{66}\end{Bmatrix} = \int_{-h/2}^{h/2} C_{11}\left(1, z, z^2, f(z), z\,f(z), f^2(z)\right)\begin{Bmatrix} 1 \\ \nu \\ \dfrac{1-\nu}{2}\end{Bmatrix} dz \\
&\left(A_{22}, B_{22}, D_{22}, B^s_{22}, D^s_{22}, H^s_{22}\right)=\left(A_{11}, B_{11}, D_{11}, B^s_{11}, D^s_{11}, H^s_{11}\right) \\
&A^s_{44}=A^s_{55}=\int_{-h/2}^{h/2} C_{44}\left[g(z)\right]^2 dz,
\end{aligned} \tag{25}$$

Substituting Eq. (19) into Eq. (18), the equations of motion can be expressed in terms of displacements (u_0 , v_0 , w_b , w_s) and the suitable equations take the following forms

$$\begin{aligned}
&A_{11}\frac{\partial^2 u_0}{\partial x^2}+A_{66}\frac{\partial^2 u_0}{\partial y^2}+\left(A_{12}+A_{66}\right)\frac{\partial^2 v}{\partial x\partial y}-B_{11}\frac{\partial^3 w_b}{\partial x^3}-\left(B_{12}+2B_{66}\right)\frac{\partial^3 w_b}{\partial x\partial y^2}-B^s_{11}\frac{\partial^3 w_s}{\partial x^3}-\left(B^s_{12}+2B^s_{66}\right)\frac{\partial^3 w_s}{\partial x\partial y^2} \\
&=I_0\ddot{u}_0-I_1\frac{\partial \ddot{w}_b}{\partial x}-J_1\frac{\partial \ddot{w}_s}{\partial x}, \\
&\left(A_{12}+A_{66}\right)\frac{\partial^2 u_0}{\partial x\partial y}+A_{66}\frac{\partial^2 v_0}{\partial x^2}+A_{22}\frac{\partial^2 v_0}{\partial y^2}-\left(B_{12}+2B_{66}\right)\frac{\partial^3 w_b}{\partial x^2\partial y}-B_{22}\frac{\partial^3 w_b}{\partial y^3}-B^s_{22}\frac{\partial^3 w_s}{\partial y^3}-\left(B^s_{12}+2B^s_{66}\right)\frac{\partial^3 w_s}{\partial x^2\partial y} \\
&=I_0\ddot{v}_0-I_1\frac{\partial \ddot{w}_b}{\partial y}-J_1\frac{\partial \ddot{w}_s}{\partial y}, \\
&B_{11}\frac{\partial^3 u}{\partial x^3}+\left(B_{12}+2B_{66}\right)\frac{\partial^3 u}{\partial x\partial y^2}+\left(B_{12}+2B_{66}\right)\frac{\partial^3 v}{\partial x^2\partial y}+B_{22}\frac{\partial^3 v}{\partial y^3}-D_{11}\frac{\partial^4 w_b}{\partial x^4}-2\left(D_{12}+2D_{66}\right)\frac{\partial^4 w_b}{\partial x^2\partial y^2}-D_{22}\frac{\partial^4 w_b}{\partial y^4} \\
&-D^s_{11}\frac{\partial^4 w_s}{\partial x^4}-2\left(D^s_{12}+2D^s_{66}\right)\frac{\partial^4 w_s}{\partial x^2\partial y^2}-D^s_{22}\frac{\partial^4 w_s}{\partial y^4}=I_0\left(\ddot{w}_b+\ddot{w}_s\right)+I_1\left(\frac{\partial \ddot{u}_0}{\partial x}+\frac{\partial \ddot{v}_0}{\partial y}\right)-I_2\nabla^2\ddot{w}_b-J_2\nabla^2\ddot{w}_s, \\
&B^s_{11}\frac{\partial^3 u}{\partial x^3}+\left(B^s_{12}+2B^s_{66}\right)\frac{\partial^3 u}{\partial x\partial y^2}+\left(B^s_{12}+2B^s_{66}\right)\frac{\partial^3 v}{\partial x^2\partial y}+B^s_{22}\frac{\partial^3 v}{\partial y^3}-D^s_{11}\frac{\partial^4 w_b}{\partial x^4}-2\left(D^s_{12}+2D^s_{66}\right)\frac{\partial^4 w_b}{\partial x^2\partial y^2}-D^s_{22}\frac{\partial^4 w_b}{\partial y^4} \\
&-H^s_{11}\frac{\partial^4 w_s}{\partial x^4}-2\left(H^s_{12}+2H^s_{66}\right)\frac{\partial^4 w_s}{\partial x^2\partial y^2}-H^s_{22}\frac{\partial^4 w_s}{\partial y^4}+A^s_{55}\frac{\partial^2 w_s}{\partial x^2}+A^s_{44}\frac{\partial^2 w_s}{\partial y^2}=I_0\left(\ddot{w}_b+\ddot{w}_s\right)+J_1\left(\frac{\partial \ddot{u}_0}{\partial x}+\frac{\partial \ddot{v}_0}{\partial y}\right) \\
&-J_2\nabla^2\ddot{w}_b-K_2\nabla^2\ddot{w}_s
\end{aligned} \tag{26a}$$

Note that as the effect of transverse shear deformation is neglected, Eq. (26a) yields the equations of motion of FG plate based on the classical plate theory (CPT). The suitable equations take the following forms

$$\begin{aligned}
&A_{11}\frac{\partial^2 u_0}{\partial x^2}+A_{66}\frac{\partial^2 u_0}{\partial y^2}+\left(A_{12}+A_{66}\right)\frac{\partial^2 v_0}{\partial x\partial y}-B_{11}\frac{\partial^3 w_b}{\partial x^3}-\left(B_{12}+2B_{66}\right)\frac{\partial^3 w_b}{\partial x\partial y^2}=I_0\ddot{u}_0 \\
&\left(A_{12}+A_{66}\right)\frac{\partial^2 u_0}{\partial x\partial y}+A_{66}\frac{\partial^2 v_0}{\partial x^2}+A_{22}\frac{\partial^2 v_0}{\partial y^2}-\left(B_{12}+2B_{66}\right)\frac{\partial^3 w_b}{\partial x^2\partial y}-B_{22}\frac{\partial^3 w_b}{\partial y^3}=I_0\ddot{v}_0 \\
&B_{11}\frac{\partial^3 u_0}{\partial x^3}+\left(B_{12}+2B_{66}\right)\frac{\partial^3 u_0}{\partial x\partial y^2}+\left(B_{12}+2B_{66}\right)\frac{\partial^3 v_0}{\partial x^2\partial y}+B_{22}\frac{\partial^3 v_0}{\partial y^3}-D_{11}\frac{\partial^4 w_b}{\partial x^4} \\
&-2\left(D_{12}+2D_{66}\right)\frac{\partial^4 w_b}{\partial x^2\partial y^2}-D_{22}\frac{\partial^4 w_b}{\partial y^4}=I_0\ddot{w}_b-I_2\nabla^2\ddot{w}_b
\end{aligned} \tag{26b}$$

3. The Solution of the Problem

The exact solution of Eqs. (26a) for the FG porous sandwich plate under various boundary conditions can be constructed. The boundary conditions for an arbitrary edge with free, simply supported and clamped edge conditions are

Table 1. The admissible functions for different boundary conditions

Boundary Conditions	$x=0$	$y=0$	$x=a$	$y=b$	$X_m(x)$	$Y_n(y)$
SSSS	S	S	S	S	$\sin(\lambda x)$	$\sin(\mu x)$
CSCS	C	S	C	S	$\sin^2(\lambda x)$	$\sin(\mu x)$
CCCC	C	C	C	C	$\sin^2(\lambda x)$	$\sin^2(\mu x)$
FCFC	F	C	F	C	$\cos^2(\lambda x)[\sin^2(\lambda x)+1]$	-

- Clamped (C)

$$u_0 = v_0 = w_b = w_s = \frac{\partial w_b}{\partial x} = \frac{\partial w_s}{\partial x} = 0 \quad \text{at} \quad x = 0, a \tag{27a}$$

$$u_0 = v_0 = w_b = w_s = \frac{\partial w_b}{\partial y} = \frac{\partial w_s}{\partial y} = 0 \quad \text{at} \quad y = 0, b \tag{27b}$$

- Simply supported (SS)

$$N_x = v_0 = w_b = w_s = M_x = 0 \quad \text{at} \quad x = 0, a \tag{28a}$$

$$u_0 = N_y = w_b = w_s = M_y = 0 \quad \text{at} \quad y = 0, b \tag{28b}$$

- Free (F)

$$N_x = N_{xy} = \frac{\partial M_x}{\partial x} + 2\frac{\partial M_{xy}}{\partial y} = Q_x = M_x = 0 \quad \text{at} \quad x = 0, a \tag{29a}$$

$$N_{xy} = N_y + 2\frac{\partial M_{xy}}{\partial y} + \frac{\partial M_y}{\partial y} = Q_y = M_y = 0 \quad \text{at} \quad y = 0, b \tag{29b}$$

In the present problem, the following expressions are considered for the displacements that satisfy the considered boundary conditions

$$\begin{Bmatrix} u_0 \\ v_0 \\ w_b \\ w_s \end{Bmatrix} = \begin{Bmatrix} U_{mn} \dfrac{\partial X_m(x)}{\partial x} Y_n(y) e^{i\omega t} \\ V_{mn} X_n(x) \dfrac{\partial Y_n(y)}{\partial y} e^{i\omega t} \\ W_{bmn} X_n(x) Y_n(y) e^{i\omega t} \\ W_{smn} X_n(x) Y_n(y) e^{i\omega t} \end{Bmatrix} \tag{30}$$

where U_{mn}, V_{mn}, W_{bmn}, and W_{smn} are arbitrary parameters and $\omega = \omega_{mn}$ indicates the eigenfrequency associated with $(m,n)^{th}$ eigenmode. The suggested functions $X_m(x)$ and $Y_n(y)$ satisfy the geometric boundary conditions given in Eqs. (27) and (28) and denote approximate shapes of the deflected surface of the sandwich plate. The admissible functions for different cases of boundary conditions are presented in Table 1, where $\lambda = m\pi / a$ and $\mu = n\pi / b$.

Substituting the Eq. (30) into the Eqs. (24), and then multiplying each equation with the suitable eigenfunction and integrating over the domain of solution, after some mathematical rearrangement the following matrix format is gotten

$$\left(\begin{bmatrix} a_{11} & a_{12} & a_{13} & a_{14} \\ a_{12} & a_{22} & a_{23} & a_{24} \\ a_{13} & a_{23} & a_{33} & a_{34} \\ a_{14} & a_{24} & a_{34} & a_{44} \end{bmatrix} - \omega^2 \begin{bmatrix} m_{11} & 0 & m_{13} & m_{14} \\ 0 & m_{22} & m_{23} & m_{24} \\ m_{31} & m_{32} & m_{33} & m_{34} \\ m_{41} & m_{42} & m_{43} & m_{44} \end{bmatrix} \right) \begin{Bmatrix} U_{mn} \\ V_{mn} \\ W_{mn} \\ X_{mn} \end{Bmatrix} = \begin{Bmatrix} 0 \\ 0 \\ 0 \\ 0 \end{Bmatrix} \tag{31}$$

in which

$$\begin{gathered} a_{11} = A_{11}\alpha_{12} + A_{66}\alpha_8, \quad a_{12} = (A_{12} + A_{66})\alpha_8, \quad a_{13} = -B_{11}\alpha_{12} - (B_{12} + 2B_{66})\alpha_8, \quad a_{14} = -(B^s_{12} + 2B^s_{66})\alpha_8 - B^s_{11}\alpha_{12} \\ a_{21} = (A_{12} + A_{66})\alpha_{10}, \quad a_{22} = A_{22}\alpha_4 + A_{66}\alpha_{10}, \quad a_{23} = -B_{22}\alpha_4 - (B_{12} + 2B_{66})\alpha_{10}, \quad a_{24} = -(B^s_{12} + 2B_{66})\alpha_{10} - B^s_{22}\alpha_4 \\ a_{31} = B_{11}\alpha_{13} + (B_{12} + 2B_{66})\alpha_{11}, \quad a_{32} = (B_{12} + 2B_{66})\alpha_{11} + B_{22}\alpha_5, \; a_{33} = -D_{11}\alpha_{13} - 2(D_{12} + 2D_{66})\alpha_{11} - D_{22}\alpha_5 \\ a_{34} = -D^s_{11}\alpha_{13} - 2(D^s_{12} + 2D^s_{66})\alpha_{11} - D^s_{66}\alpha_5, \\ a_{41} = B^s_{11}\alpha_{13} + (B^s_{12} + 2B^s_{66})\alpha_{11}, \quad a_{42} = (B^s_{12} + 2B^s_{66})\alpha_{11} + B^s_{22}\alpha_5, \\ a_{43} = -D^s_{11}\alpha_{13} - 2(D^s_{12} + 2D^s_{66})\alpha_{11} - D^s_{22}\alpha_5, \; a_{44} = -H^s_{11}\alpha_{13} - 2(H^s_{12} + 2H^s_{66})\alpha_{11} - H^s_{22}\alpha_5 + A^s_{44}\alpha_9 + A^s_{55}\alpha_3 \end{gathered} \tag{32}$$

and

$$\begin{gathered} m_{11}=-I_0\alpha_6\,,\;\; m_{13}=-I_1\alpha_6\,,\;\; m_{14}=J_1\alpha_6 \\ m_{22}=-I_0\alpha_2\,,\;\; m_{23}=I_1\alpha_2\,,\;\; m_{24}=J_1\alpha_2 \\ m_{31}=-I_1\alpha_9\,,\;\; m_{32}=-I_1\alpha_3\,,\;\; m_{33}=-I_0\alpha_1+I_2\left(\alpha_3+\alpha_9\right),\;\; m_{34}=-I_0\alpha_1+J_2\left(\alpha_3+\alpha_9\right) \\ m_{41}=-J_1\alpha_9\,,\;\; m_{42}=-J_1\alpha_3\,,\;\; m_{44}=-I_0\alpha_1+K_2\left(\alpha_3+\alpha_9\right) \end{gathered} \tag{33}$$

with

$$\begin{gathered} \left(\alpha_1,\alpha_3,\alpha_5\right)=\int_0^b\int_0^a\left(X_mY_n,X_mY_n'',X_mY_n''''\right)X_mY_n dxdy\,,\;\; \left(\alpha_2,\alpha_4,\alpha_{10}\right)=\int_0^b\int_0^a\left(X_mY_n',X_mY_n''',X_m''Y_n'\right)X_mY_n' dxdy \\ \left(\alpha_6,\alpha_8,\alpha_{12}\right)=\int_0^b\int_0^a\left(X_m'Y_n,X_m'Y_n'',X_m'''Y_n\right)X_m'Y_n dxdy\,,\;\; \left(\alpha_7,\alpha_9,\alpha_{11},\alpha_{13}\right)=\int_0^b\int_0^a\left(X_m'Y_n',X_m''Y_n,X_m'Y_n'',X_m''''Y_n\right)X_mY_n dxdy \end{gathered} \tag{34}$$

The nontrivial solution is gotten as the determinant of Eq. (31) equals zero.

4. Numerical Results and Discussion

In this section, several parametrical studies are performed for examining the effects of the porosity, geometry parameters, and boundary conditions on the free vibration of the FG porous sandwich plates. It is supposed that the FG porous sandwich plate composed of (Al) as metal and (Al_2O_3) as ceramic. The material properties are taken to be E_m=70 GPa, νm=0.3, $\rho_m=2702kg/m^3$, E_c=380 GPa, ν_c=0.3, $\rho_c=3800kg/m^3$ and the following dimensionless form is used: $\bar{\omega}=\omega\, a^2\sqrt{\rho_0/E_0}/h$ where $E_0=1GPa,\rho_0=1kg/m^3$.

The following lay-up schemes are considered for FG porous sandwich plate

Scheme (1-0-1): The sandwich plate has two face layers with equal thickness while it does not include a core $h_1= h_3= h/2$, $h_2=0$
Scheme (1-1-1): The sandwich plate has three layers with equal thickness $h_1=h_2=h_3=h/3$
Scheme (1-2-1): The sandwich plate has a core layer with the twice thickness of face layers $h_1=h_3=h/4$, $h_2= h/2$
Scheme (2-1-2): The sandwich plate has a core layer with the half of thickness of face layers $h_1=h_3=2h/5$, $h_2=h/5$
Scheme (2-2-1): The sandwich plate has a core layer with the twice upper face layer while the same as the lower one $h_1=h_2=2h/5$, $h_3=h/5$.

Table 2. The comparison of the dimensionless fundamental frequencies of FG sandwich square plate versus varying power-law index

k	Theory	Scheme				
		1-0-1	2-1-2	1-1-1	2-2-1	1-2-1
0	3D (Li et al. [65])	1.8268	1.8268	1.8268	1.8268	1.8268
	HSDT (El Meiche et al. [66])	1.8245	1.8245	1.8245	1.8245	1.8245
	SSDPT (Zenkour [13])	1.8245	1.8245	1.8245	1.8245	1.8245
	TSDPT (Zenkour [13])	1.8245	1.8245	1.8245	1.8245	1.8245
	FSDPT (Zenkour [13])	1.8244	1.8244	1.8244	1.8244	1.8244
	FSDPT (Thai [67])	1.8244	1.8244	1.8244	1.8244	1.8244
	Present	1.8245	1.8245	1.8245	1.8245	1.8245
0.5	3D (Li et al. [65])	1.4461	1.4861	1.5213	1.5493	1.5767
	HSDT (El Meiche et al. [66])	1.4442	1.4841	1.5192	1.5471	1.5746
	SSDPT (Zenkour [13])	1.4444	1.4842	1.5193	1.5520	1.5745
	TSDPT (Zenkour [13])	1.4442	1.4841	1.5192	1.5520	1.5727
	FSDPT (Zenkour [13])	1.4417	1.4816	1.5170	1.5500	1.5727
	FSDPT (Thai [67])	1.4442	1.4841	1.5192	1.5471	1.5745
	Present	1.4447	1.4844	1.5195	1.5474	1.5747
1	3D (Li et al. [65])	1.2447	1.3018	1.3552	1.3976	1.4414
	HSDT (El Meiche et al. [66])	1.2431	1.3000	1.3533	1.3956	1.4394
	SSDPT (Zenkour [13])	1.2434	1.3002	1.3534	1.4079	1.4393
	TSDPT (Zenkour [13])	1.2432	1.3001	1.3533	1.4079	1.4393
	FSDPT (Zenkour [13])	1.2403	1.2973	1.3507	1.4056	1.4372
	FSDPT (Thai [67])	1.2429	1.3000	1.3533	1.3956	1.4393
	Present	1.2438	1.3006	1.3537	1.3959	1.4396
5	3D (Li et al. [65])	0.9448	0.9810	1.0453	1.1098	1.1757
	HSDT (El Meiche et al. [66])	0.9457	0.9817	1.0446	1.1088	1.1740
	SSDPT (Zenkour [13])	0.9463	0.9821	1.0448	1.1474	1.1740
	TSDPT (Zenkour [13])	0.9460	0.9818	1.0447	1.1473	1.1740
	FSDPT (Zenkour [13])	0.9426	0.9787	1.0418	1.1447	1.1716
	FSDPT (Thai [67])	0.9431	0.9796	1.0435	1.1077	1.1735
	Present	0.9469	0.9825	1.0452	1.1095	1.1744
10	3D (Li et al. [65])	0.9273	0.9408	0.9952	1.0610	1.1247
	HSDT (El Meiche et al. [66])	0.9281	0.9428	0.9954	1.0608	1.1231
	SSDPT (Zenkour [13])	0.9288	0.9433	0.9952	1.0415	1.1346
	TSDPT (Zenkour [13])	0.9284	0.9430	0.9955	1.1053	1.1231
	FSDPT (Zenkour [13])	0.9251	0.9396	0.9926	1.1026	1.1207
	FSDPT (Thai [67])	0.9246	0.9390	0.9932	1.0587	1.1223
	Present	0.9294	0.9437	0.9961	1.0616	1.1236

Table 3. The comparison of the dimensionless fundamental frequencies of FG sandwich square plate with hardcore versus varying power-law index

k	Results	Scheme				
		1-0-1	2-1-2	1-1-1	2-2-1	1-2-1
0	3D (Li et al. [65])	1.6771	1.6771	1.6771	1.6771	1.6771
	FSDPT (Thai [67])	1.6697	1.6697	1.6697	1.6697	1.6697
	Present	1.6703	1.6703	1.6703	1.6703	1.6703
0.5	3D (Li et al. [65])	1.3536	1.3905	1.4218	1.4454	1.4694
	FSDPT (Thai [67])	1.3473	1.3841	1.4152	1.4386	1.4626
	Present	1.3481	1.3847	1.4155	1.4389	1.4627
1	3D (Li et al. [65])	1.1749	1.2292	1.2777	1.3143	1.3534
	FSDPT (Thai [67])	1.1691	1.2232	1.2714	1.3078	1.3467
	Present	1.1706	1.2241	1.2719	1.3082	1.3469
5	3D (Li et al. [65])	0.8909	0.9336	0.9980	1.0561	1.1190
	FSDPT (Thai [67])	0.8853	0.9286	0.9916	1.0488	1.1118
	Present	0.8960	0.9370	0.9963	1.0535	1.1136
10	3D (Li et al. [65])	0.8683	0.8923	0.9498	1.0095	1.0729
	FSDPT (Thai [67])	0.8599	0.8860	0.9428	1.0012	1.0648
	Present	0.8733	0.9004	0.9513	1.0098	1.0681

Table 4. The comparison of the dimensionless fundamental frequencies of FG sandwich square plate with softcore versus varying power-law index

k	Results	Scheme				
		1-0-1	2-1-2	1-1-1	2-2-1	1-2-1
0	3D (Li et al. [65])	0.8529	0.8529	0.8529	0.8529	0.8529
	FSDPT (Thai [67])	0.8491	0.8491	0.8491	0.8491	0.8491
	Present	0.8501	0.8501	0.8501	0.8501	0.8501
0.5	3D (Li et al. [65])	1.3789	1.3206	1.2805	1.2453	1.2258
	FSDPT (Thai [67])	1.3686	1.3115	1.2729	1.2380	1.2185
	Present	1.3806	1.3255	1.2834	1.2493	1.2243
1	3D (Li et al. [65])	1.5090	1.4333	1.3824	1.3420	1.3213
	FSDPT (Thai [67])	1.4915	1.4156	1.3702	1.3302	1.3104
	Present	1.5146	1.4509	1.3988	1.3593	1.3257
5	3D (Li et al. [65])	1.6587	1.5801	1.5028	1.4601	1.4267
	FSDPT (Thai [67])	1.6305	1.5125	1.4589	1.4195	1.4026
	Present	1.6568	1.6127	1.5586	1.5162	1.4666
10	3D (Li et al. [65])	1.6728	1.6091	1.5267	1.4831	1.4410
	FSDPT (Thai [67])	1.6495	1.5196	1.4642	1.4266	1.4101
	Present	1.6671	1.6349	1.5856	1.5436	1.4928

4.1. Comparison Studies

Comparison 1: For validation of results three comparison studies are performed. In Table 2 the variation of fundamental frequencies of FG sandwich square plate with SSSS boundary conditions versus different lay-up schemes and power-law index are tabulated and compared with the results of Zenkour [13] based on sinusoidal shear deformation plate theory (SSDPT), trigonometric shear deformation plate theory (TSDPT) and first-order shear deformation plate theory (FSDPT), Li et al. [65] based on the three-dimensional (3D) solutions, El Meiche et al. [66] based on the hyperbolic shear deformation plate theory (HSDPT), and Thai et al. [67] based on the first-order shear deformation (FSDPT) for a/h=10. As seen from Tables 2 present results are in good agreement with the previously published ones. Besides, as the present theory includes only four unknowns in contrast to the five unknowns in the SSDPT, TSDPT and FSDPT make the present formulation more valuable.

Comparison 2: Tables 3 and 4 present the variation of dimensionless fundamental frequencies of FG sandwich square plate with SSSS boundary conditions versus different lay-up schemes and power-law index, here side to thickness ratio taken to be a/h=5 as well as two cases of FG sandwich plates are considered a ceramic core (hardcore) in Table 3 and a metal core (softcore) in Table 4. Dimensionless fundamental frequencies are compared with exact 3D solutions by Li et al. [61] and the first-order shear deformation of Thai et al. [63]. As it is seen from Tables 3 and 4 present results are in good agreement with the previously published ones.

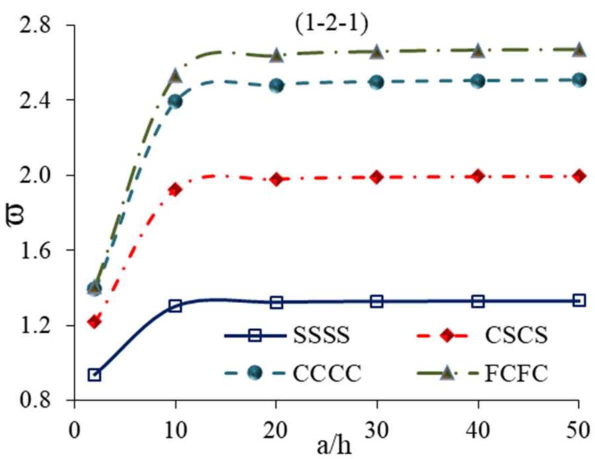

Fig 2. The variation of the dimensionless fundamental frequency of FG sandwich square plate versus side to thickness ratio

Table 5. The variation of the dimensionless fundamental frequencies of FG sandwich square plate versus varying power-law index under different boundary conditions

Boundary Conditions	k	Scheme 1-0-1	2-1-2	1-1-1	2-2-1	1-2-1
SSSS	0	1.8245	1.8245	1.8245	1.8245	1.8245
	0.5	1.4447	1.4844	1.5195	1.5474	1.5747
	1	1.2438	1.3006	1.3537	1.3959	1.4396
	2	1.0622	1.1229	1.1889	1.2443	1.3028
	5	0.9469	0.9825	1.0452	1.1095	1.1744
	10	0.9294	0.9437	0.9961	1.0616	1.1236
CSCS	0	2.6703	2.6703	2.6703	2.6703	2.6703
	0.5	2.1287	2.1869	2.2375	2.2772	2.3165
	1	1.8382	1.9221	1.9993	2.0599	2.1231
	2	1.5733	1.6642	1.7607	1.8408	1.9259
	5	1.4023	1.4588	1.5514	1.6448	1.7399
	10	1.3731	1.4014	1.47953	1.5749	1.6661
CCCC	0	3.2942	3.2942	3.2942	3.2942	3.2942
	0.5	2.6389	2.7109	2.7727	2.8205	2.8684
	1	2.2839	2.3881	2.4829	2.5566	2.6337
	2	1.9580	2.0719	2.1911	2.2890	2.3935
	5	1.7450	1.8188	1.9339	2.0485	2.1659
	10	1.7056	1.7476	1.8453	1.9624	2.0753
FCFC	0	3.4696	3.4696	3.4696	3.4696	3.4696
	0.5	2.7889	2.8646	2.9292	2.9789	3.0288
	1	2.4175	2.5276	2.6271	2.7039	2.7846
	2	2.0749	2.1962	2.3217	2.4241	2.5338
	5	1.8491	1.9299	2.0516	2.1719	2.2955
	10	1.8051	1.8545	1.9583	2.0813	2.2004

4.2. Parametric Studies

Study 1: In the first study the effects of boundary conditions on the dimensionless fundamental frequencies of FG sandwich square plates are examined. For this aim, the variations of the dimensionless fundamental frequencies of FG sandwich square plate versus different lay-up schemes and power-law index are presented under different boundary conditions in Table 5, where side to thickness ratio is taken to be a/h=10. Furthermore, the variation of the dimensionless fundamental frequency of FG sandwich square plate with lay-up scheme (1-2-1) versus side to thickness ratio is illustrated in Fig. 2, here the power-law index taken to be k=2. It is seen that the highest values of dimensionless fundamental frequencies of FG sandwich plates occur in FCFC boundary conditions while the lowest ones occur in SSSS boundary conditions.

Study 2: In the second study, the dimensionless fundamental frequencies of FG sandwich square plate with SSSS boundary conditions versus different lay-up schemes and power-law index are presented in Fig. 3, where side to thickness ratio is taken to be a/h=10. It is seen that the values of the dimensionless fundamental frequency of the FG sandwich square plate decrease with the increase of the power-law index, because increasing the power-law index reduces the stiffness of the FG sandwich plate.

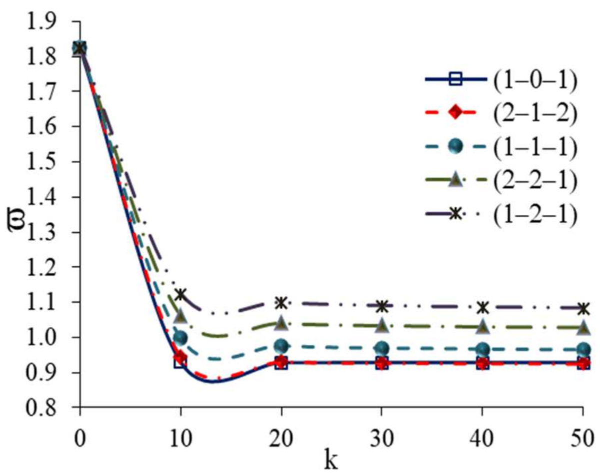

Fig 3. The variation of the dimensionless fundamental frequency of FG sandwich square plate versus power-law index

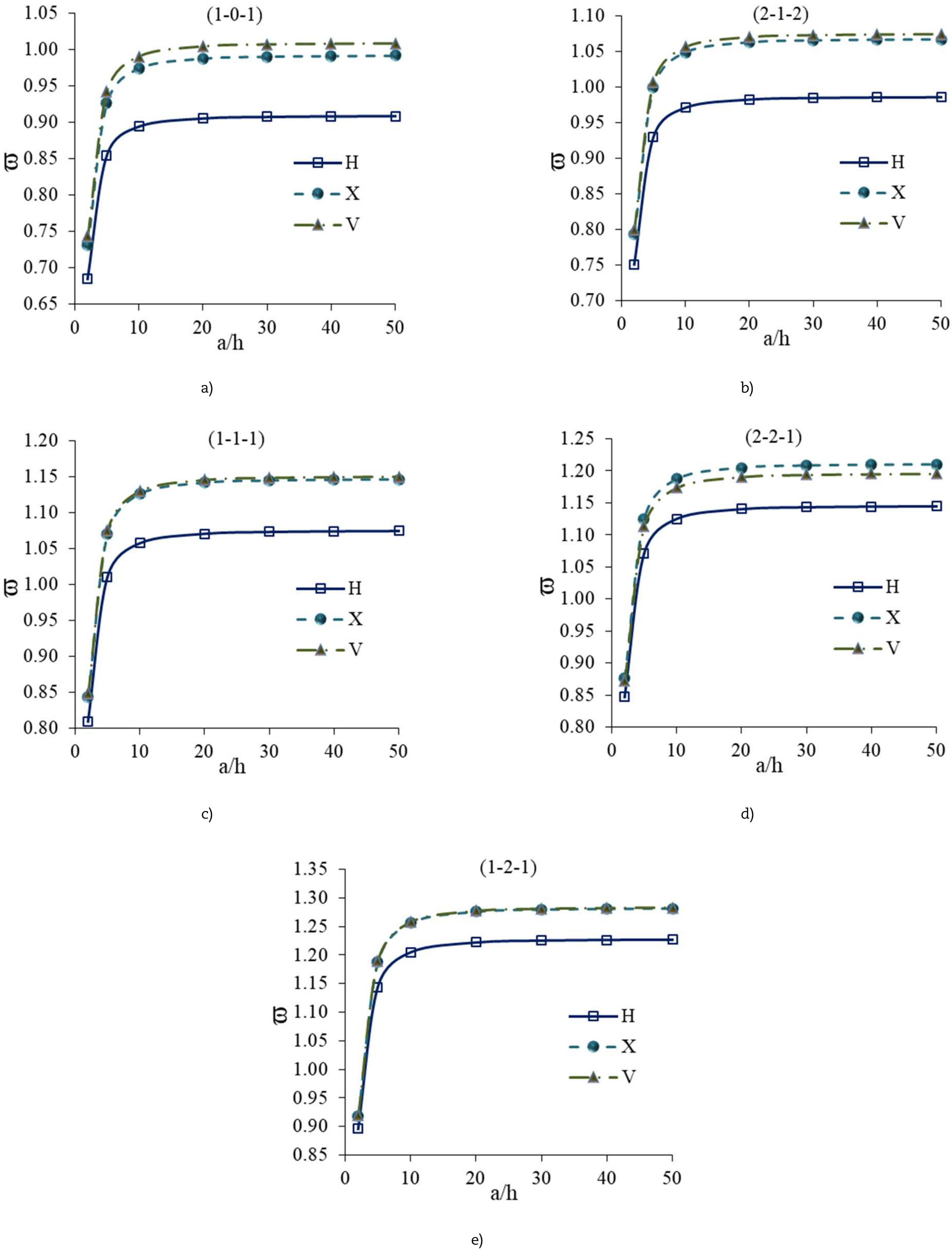

Fig 4. The variation of the dimensionless fundamental frequency of FG porous sandwich square plate versus side to thickness ratio

Study 3: In the third study, the effects of the type of porosity model and side to thickness ratio are examined. For this purpose, the variation of the dimensionless fundamental frequency of FG porous sandwich square plate with SSSS boundary conditions versus different porosity models and side to thickness ratio is plotted for different layup schemes in Fig. 4, where power-law index and porosity volume fraction are taken to be k=2 and ξ=0.2, respectively. It is observed that the difference between the porosity models increases with the increasing of side to thickness ratio. Especially, for high values of side to thickness ratio the type of porosity distributions model plays an important role in the free vibration behavior of FG porous sandwich plates. In all lay-up schemes, the homogeneous (H) porosity model has the lowest dimensionless fundamental frequencies. The reason for this situation is that the void more stack in the H porosity distribution, and so the rigidity of the plate becomes the lowest in the H porosity model.

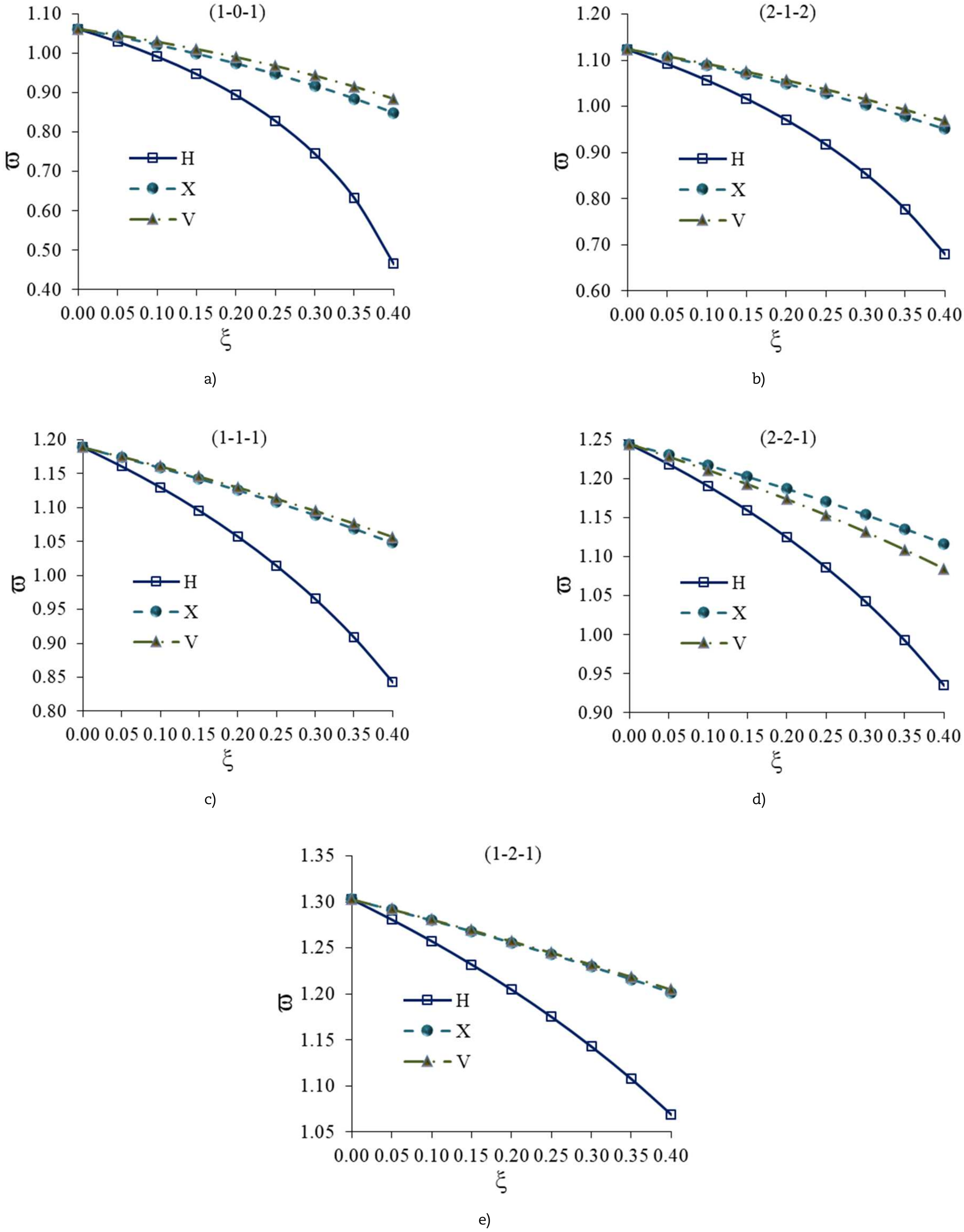

Fig 5. The variation of the dimensionless fundamental frequency of FG porous sandwich square plate versus porosity volume fraction

Study 4: In the fourth study, the effects of the type of porosity model and porosity volume fraction ratio are examined. For this aim, the variation of the dimensionless fundamental frequency of FG porous sandwich square plate with SSSS boundary conditions versus different porosity models and porosity volume fractions are illustrated for different layup schemes in Fig. 5, where power-law index and side to thickness ratio are taken to be k=2 and a/h=10, respectively. It is obtained that the difference between the porosity models increases with increasing porosity volume fraction. In all lay-up schemes, the H porosity model has the lowest dimensionless fundamental frequencies. Besides, the values of dimensionless fundamental frequencies of X and V porosity models are very close to each other in (1-1-1) and (1-2-1) schemes while they are very distinct from those for (1-0-1), (2-1-2) and (2-2-1) lay-up schemes.

5. Conclusions

In this study, free vibration analysis of the square sandwich plate with FG porous face sheets and isotropic homogenous core was performed under various boundary conditions. To this end, the material properties of the sandwich plate were supposed to vary continuously through the thickness direction according to the volume fraction of constituents defined with the modified rule of the mixture including porosity volume fraction with three different types of porosity distribution over the cross-section. Furthermore, a hyperbolic shear displacement theory was used in the kinematic relation of the FG porous sandwich plate, and the equations of motion were derived utilizing Hamilton's principle. Analytical solutions were obtained for free vibration analysis of square sandwich plates with FG porous layers under various boundary conditions. Several parametrical studies were performed for examining the effects of the porosity volume fraction, type of porosity distribution model, lay-up scheme, side to thickness ratio, and boundary conditions on the free vibration of the FG sandwich plates.

Briefly, the following results were obtained:

- The highest values of dimensionless fundamental frequencies of FG sandwich plates occur in FCFC boundary conditions while the lowest ones occur in SSSS boundary conditions
- The values of the dimensionless fundamental frequency of FG sandwich plate decrease with the increase of the power-law index
- The type of porosity distribution model plays an important role in the free vibration behavior of FG porous sandwich plates, especially for high values of side to thickness ratio.
- In all lay-up schemes, the homogenous porosity model has the lowest the dimensionless fundamental frequencies
- The difference between the porosity models increases with the increase of porosity volume fraction.

Finally, it was concluded that the types of adopted porosity distribution model, porosity volume fraction, lay-up scheme, side to thickness ratio, and boundary conditions have significant effects on the free vibration of the FG sandwich plates. The negative effects of porosity may be reduced by adopting suitable values for said parameters, considerably.

Author Contributions

Lazreg Hadji planned the scheme, initiated the project, and developed the mathematical modeling. Mehmet Avcar examined the theory validation and analyzed the results. The manuscript was written through the contribution of all authors. All authors discussed the results, reviewed, and approved the final version of the manuscript.

Conflict of Interest

The authors declared no potential conflicts of interest with respect to the research, authorship, and publication of this article.

References

[1] Koizumi, M., FGM activities in Japan, *Composites Part B: Engineering*, 28(1-2), 1997, 1–4.
[2] Kieback, B., Neubrand, A., Riedel, H., Processing techniques for functionally graded materials, *Materials Science and Engineering*: A, 362(1-2), 2013, 81-106.
[3] Naebe, M., Shirvanimoghaddam, K., Functionally graded materials: A review of fabrication and properties, *Applied Materials Today*, 5, 2016, 223-245.
[4] Civalek Ö, Free vibration of carbon nanotubes reinforced (CNTR) and functionally graded shells and plates based on FSDT via discrete singular convolution method, *Composites Part B: Engineering*, 111, (2017), 45-59.
[5] Avcar, M., Mohammed, W.K.M., Free vibration of functionally graded beams resting on Winkler-Pasternak foundation, *Arabian Journal of Geosciences*, 11(10), 2018, 232.
[6] Larbi, L.O., Hadji, L., Meziane, M.A.A., Adda Bedia, E.A., An analytical solution for free vibration of functionally graded beam using a simple first-order shear deformation theory, *Wind and Structures*, 27(4), 2018, 247-254.
[7] Sahouane, A., Hadji, L., Bourada, M., Numerical analysis for free vibration of functionally graded beams using an original HSDBT, *Earthquakes and Structures*, 17(1), 2019, 31-37.
[8] Akbaş, S.D., Forced vibration responses of axially functionally graded beams by using Ritz method, Journal *of Applied and Computational Mechanics*, 2020, https://doi.org/10.22055/JACM.2020.34865.2491
[9] Alsaid-Alwan H.H.S, Avcar M., Analytical solution of free vibration of FG beam utilizing different types of beam theories: A comparative study, *Computers and Concrete* 26(3), 2020, 285-292.
[10] Civalek, Ö., Avcar, M, Free vibration and buckling analyses of CNT reinforced laminated non-rectangular plates by discrete singular convolution method, *Engineering with Computers*, 2020, 1-33. https://doi.org/10.1007/s00366-020-01168-8
[11] Vinson J.R., *Sandwich Structures: Past, Present, and Future*, In: Thomsen O., Bozhevolnaya E., Lyckegaard A. (eds) Sandwich Structures 7: Advancing with Sandwich Structures and Materials, Springer, Dordrecht, 2005.
[12] Zenkour, A.M., A comprehensive analysis of functionally graded sandwich plates: Part 1—Deflection and stresses, *International Journal of Solids and Structures*, 42(18-19), 2005a, 224-5242.
[13] Zenkour, A.M., A comprehensive analysis of functionally graded sandwich plates: Part 2—Buckling and free vibration, *International Journal of Solids and Structures*, 42(18-19), 2005b,5243-5258.
[14] Zenkour, A.M., Sobhy, M., Thermal buckling of various types of FGM sandwich plates, *Composite Structures*, 93(1), 2010, 93-102.
[15] El Meiche, N., Tounsi, A., Ziane, N., Mechab, I. , A new hyperbolic shear deformation theory for buckling and vibration of functionally graded sandwich plate, *International Journal of Mechanical Sciences*, 53(4), 2011, 237-247.
[16] Mohammadi, Y., Khalili, S.M.R., *Free Vibration Analysis of Sandwich Plates with Temperature-Dependent Properties of the Core Materials and Functionally Graded Face Sheets*, In Mechanics and Properties of Composed Materials and Structures (pp. 183-197), Springer, Berlin, Heidelberg, 2012.
[17] Bessaim, A., Houari, M.S., Tounsi, A., Mahmoud, S. R., Bedia, E.A.A., A new higher-order shear and normal deformation theory for the static and free vibration analysis of sandwich plates with functionally graded isotropic face sheets, *Journal of Sandwich Structures and Materials*, 15(6), 2013, 671-703.
[18] Thai, H.T., Nguyen, T.K., Vo, T.P., Lee, J., Analysis of functionally graded sandwich plates using a new first-order shear deformation theory, *European Journal of Mechanics-A/Solids*, 45, 2014, 211-225.
[19] Tlidji, Y., Daouadji, T. H., Hadji, L., Tounsi, A., Bedia, E.A.A, Elasticity solution for bending response of functionally graded sandwich plates under thermomechanical loading, *Journal of Thermal Stresses*, 37(7), 2014, 852-869.
[20] Yang, Y., Lam, C.C., Kou, K.P., Iu, V.P., Free vibration analysis of the functionally graded sandwich beams by a mesh free boundary-domain integral equation method, *Composite Structures*, 117, 2014, 32-39.
[21] Mantari, J.L., Granados, E.V., A refined FSDT for the static analysis of functionally graded sandwich plates, *Thin-Walled Structures*, 90, 2015, 24(5), 2017, 523-536.
[22] Tounsi, A., Houari, M.S.A., Bessaim, A., A new 3-unknowns non-polynomial plate theory for buckling and vibration of functionally graded sandwich plate, *Structural Engineering and Mechanics*, 60(4), 2016, 547-565.

[23] Ahmadi, I., A Galerkin layerwise formulation for three-dimensional stress analysis in long sandwich plates, *Steel and Composite Structures*, 24(5), 2017, 523-536.
[24] Menasria, A., Bouhadra, A., Tounsi, A., Bousahla, A.A., Mahmoud, S.R., A new and simple HSDT for thermal stability analysis of FG sandwich *Steel and Composite Structures*, 24(5), 2017, plates, *Steel and Composite Structures*, 25(2), 2017, 157-175.
[25] Şimşek, M., Al-Shujairi, M., Static, free and forced vibration of functionally graded (FG) sandwich beams excited by two successive moving harmonic loads, *Composites Part B: Engineering*, 108, 2017, 18-34.
[26] Wang, Q., Cui, X., Qin, B., Liang, Q., Tang, J., A semi-analytical method for vibration analysis of functionally graded (FG) sandwich doubly-curved panels and shells of revolution, *International Journal of Mechanical Sciences*, 134, 2017, 479-499.
[27] Dash, S., Mehar, K., Sharma, N., Mahapatra, T.R., Panda, S.K., Modal analysis of FG sandwich doubly curved shell structure, *Structural Engineering and Mechanics*, 68(6), 2018, 721-733.
[28] Raissi, H., Shishehsaz, M., Moradi, S., Stress distribution in a five-layer sandwich plate with FG face sheets using layerwise method, *Mechanics of Advanced Materials and Structures*, 26(14), 2019, 1234-1244.
[29] Rezaiee-Pajand, M., Arabi, E., Masoodi, A.R., Nonlinear analysis of FG-sandwich plates and shells, *Aerospace Science and Technology*, 87, 2019, 178-189.
[30] Meksi, R., Benyoucef, S., Mahmoudi, A., Tounsi, A., Adda Bedia, E. A., Mahmoud, S.R., An analytical solution for bending, buckling and vibration responses of FGM sandwich plates, *Journal of Sandwich Structures and Materials*, 21(2), 2020, 727-757.
[31] Nam, P.V., Kien, N.D., Free vibration of FG sandwich plates partially supported by elastic foundation using a quasi-3D finite element formulation, *Vietnam Journal of Mechanics*, 42(1), 2020, 63-86.
[32] Zhu, J., Lai, Z., Yin, Z., Jeon, J., Lee, S., Fabrication of ZrO2–NiCr functionally graded material by powder metallurgy, *Materials Chemistry and Physics*, 68, 2001, 130–135.
[33] Wattanasakulpong, N., Ungbhakorn, V., Linear and nonlinear vibration analysis of elastically restrained ends FGM beams with porosities, *Aerospace Science and Technology*, 32(1), 2014, 111-120.
[34] Ait Atmane, H., Tounsi, A., Bernard, F., Effect of thickness stretching and porosity on mechanical response of a functionally graded beams resting on elastic foundations, *International Journal of Mechanics and Materials in Design*, 13(1), 2017, 71–84.
[35] Ebrahimi, F., Jafari, A., A higher-order thermomechanical vibration analysis of temperature-dependent FGM beams with porosities, *Journal of Engineering*, 2016, 2016, 9561504.
[36] Akbaş, Ş.D., Vibration and static analysis of functionally graded porous plates, *Journal of Applied and Computational Mechanics*, 3(3), 2017, 199-207.
[37] Akbaş, Ş.D., Stability of a non-homogenous porous plate by using generalized differential quadrature method, *International Journal of Engineering and Applied Sciences*, 9(2), 2017, 147-147.
[38] Akbaş, Ş.D., Nonlinear static analysis of functionally graded porous beams under thermal effect, *Coupled Systems Mechanics*, 6(4), 2017, 399-415.
[39] Akbaş, Ş.D., Geometrically nonlinear analysis of functionally graded porous beams, *Wind and Structures*, 27(1), 2018, 59-70.
[40] Akbaş, Ş.D., Longitudinal forced vibration analysis of porous a nanorod, *Journal of Engineering Sciences and Design*, 7(4), 2019, 736-743.
[41] Zouatnia, N., Hadji, L., Kassoul, A., An analytical solution for bending and vibration responses of functionally graded beams with porosities, *Wind and Structures*, 25(4), 2017, 329-342.
[42] Arshid, E., Khorshidvand, A.R., Free vibration analysis of saturated porous FG circular plates integrated with piezoelectric actuators via differential quadrature method, *Thin-Walled Structures*, 125, 2018, 220-233.
[43] Wu, D., Liu, A., Huang, Y., Huang, Y., Pi, Y., Gao, W., Dynamic analysis of functionally graded porous structures through finite element analysis, *Engineering Structures*, 165, 2018, 87-301.
[44] Avcar, M., Free vibration of imperfect sigmoid and power law functionally graded beams, *Steel and Composite Structures*, 30(6), 2019, 2603-615.
[45] Chen, D., Yang, J., Kitipornchai, S., Buckling and bending analyses of a novel functionally graded porous plate using Chebyshev-Ritz method, *Archives of Civil and Mechanical Engineering*, 19(1), 2019, 157-170.
[46] Jalaei, M., Civalek, O., On dynamic instability of magnetically embedded viscoelastic porous FG nanobeam, *International Journal of Engineering Science*, 143, 2019, 14-32.
[47] Nguyen, L.B., Nguyen, N.V., Thai, C.H., Ferreira, A.M.J., Nguyen-Xuan, H., An isogeometric Bézier finite element analysis for piezoelectric FG porous plates reinforced by graphene platelets, *Composite Structures*, 214, 2019, 227-245.
[48] Arefi, M., Saeed , F., Bidgoli, EMR., Civalek, Ö., Analysis of porous micro -plates reinforced with FG-GNPs based on Reddy plate theory, *Composites Structures*, 247, 2020, 112391.
[49] Mashat, D.S., Zenkour, A.M., Radwan, A.F., A quasi 3-D higher-order plate theory for bending of FG plates resting on elastic foundations under hygro-thermo-mechanical loads with porosity, *European Journal of Mechanics-A/Solids*, 2020, 103985.
[50] Zine, A., Bousahla, A.A., Bourada, F., Benrahou, K.H., Tounsi, A., Adda Bedia, E.A., Mahmoud, S.R., Tounsi, A., Bending analysis of functionally graded porous plates via a refined shear deformation theory, *Computers and Concrete*, 26(1), 2020, 63-74.
[51] Chen, D., Kitipornchai, S., Yang, J., Nonlinear free vibration of shear deformable sandwich beam with a functionally graded porous core, *Thin-Walled Structures*, 107, 2016, 39-48.
[52] Rezaei, A.S., Saidi, A.R., Application of Carrera unified formulation to study the effect of porosity on natural frequencies of thick porous–cellular plates, *Composites Part B: Engineering*, 91, 2016, 361-370.
[53] Fazzolari, F.A., Generalized exponential, polynomial and trigonometric theories for vibration and stability analysis of porous FG sandwich beams resting on elastic foundations, *Composites Part B: Engineering*, 136, 2018, 254-271.
[54] Fu, T., Chen, Z., Yu, H., Wang, Z., Liu, X., An analytical study of sound transmission through corrugated core FGM sandwich plates filled with porous material, *Composites Part B: Engineering*, 151, 2018, 161-172.
[55] Zenkour, A.M., A quasi-3D refined theory for functionally graded single-layered and sandwich plates with porosities, *Composite Structures*, 201, 2018, 38-48.
[56] Daikh, A.A., Zenkour, A.M., Effect of porosity on the bending analysis of various functionally graded sandwich plates, *Materials Research Express*, 6(6), 2019, 065703.
[57] Heshmati, M., Jalali, S.K., Effect of radially graded porosity on the free vibration behavior of circular and annular sandwich plates, *European Journal of Mechanics-A/Solids*, 74, 2019, 417-430.
[58] Keddouri, A., Hadji, L., Tounsi, A., Static analysis of functionally graded sandwich plates with porosities, *Advances in Materials Research*, 8(3), 2019, 155-177.
[59] Rahmani, M., Mohammadi, Y., Kakavand, F., Vibration analysis of different types of porous FG circular sandwich plates, *ADMT Journal*, 12(3), 2019, 63-75.
[60] Trinh, M.C., Nguyen, D.D., Kim, S.E., Effects of porosity and thermomechanical loading on free vibration and nonlinear dynamic response of functionally graded sandwich shells with double curvature, *Aerospace Science and Technology*, 87, 2019, 119-132.
[61] Adhikari, B., Dash, P., Singh, B.N., Buckling analysis of porous FGM sandwich plates under various types nonuniform edge compression based on higher order shear deformation theory, *Composite Structures*, 251, 2020, 112597.
[62] Hadji, L., Influence of the distribution shape of porosity on the bending of FGM beam using a new higher order shear deformation model, *Smart Structures and Systems*, 26(2), 2020, 253-262.
[63] Wang, Y., Zhou, A., Fu, T., Zhang, W., Transient response of a sandwich beam with functionally graded porous core traversed by a non-uniformly distributed moving mass, *International Journal of Mechanics and Materials in Design*, 16(3), 2020, 519-540.
[64] Zhang, Y., Jin, G., Chen, M., Ye, T., Yang, C., Yin, Y., Free vibration and damping analysis of porous functionally graded sandwich plates with a viscoelastic core, *Composite Structures*, 244, 2020, 112298.
[65] Li, Q., Iu, V.P., Kou, K.P, Three-dimensional vibration analysis of functionally graded material sandwich plates, *Journal of Sound and Vibration,* 311(1-2), 2008, 498-515.
[66] El Meiche, N., Tounsi, A., Ziane, N., Mechab, I., A new hyperbolic shear deformation theory for buckling and vibration of functionally graded sandwich plate, *International Journal of Mechanical Sciences*, 53(4), 2011, 237-247.
[67] Thai, H.T., Nguyen, T.K., Vo, T.P., Lee, J., Analysis of functionally graded sandwich plates using a new first-order shear deformation theory, *European Journal of Mechanics-A/Solids*, 45, 2014, 211-225.

ORCID iD

Lazreg Hadji https://orcid.org/0000-0002-3333-5902
Mehmet Avcar https://orcid.org/ 000-0002-0689-0601

How to cite this article: Hadji L., Avcar M. Free Vibration Analysis of FG Porous Sandwich Plates under Various Boundary Conditions, *J. Appl. Comput. Mech.*, 7(2), 2021, 505–519. https://doi.org/10.22055/JACM.2020.35328.2628